^3J(H–H) = 7.6 Hz, 1 H, CHPh), 6.8–7.5 (m, Ph); ^{13}C NMR (C_6D_6) δ 27.56 (s, Me), 46.04 (d, ^1J(C–P) = 39.3 Hz, PCH_2), 51.9 (s, CMe_3), 53.43 (d, ^2J(C–P) = 9.6 Hz, *C*HPh), 198.12 (d, ^2J(C–P) = 7.0 Hz, cis CO); IR (decalin) ν(CO) 2070 (w), 1950 (m), 1940 (vs) cm^{-1}; mass spectrum (^{184}W), *m/z* (relative intensity) 607 (M^+, 26), 523 (M – 3CO, 26), 467 (M – 5CO, 80), 363 (WP(Ph)NC_4H_9, 100). Anal. Calcd for $C_{23}H_{22}NO_5PW$: C, 45.49; H, 3.65. Found: C, 45.30; H, 3.64.

11b: colorless solid, mp 104 °C; ^{31}P NMR (C_6D_6) δ 127.5 ($^1J(^{31}P–^{183}W)$ = 278 Hz); ^{1}H NMR (C_6D_6) δ 1.06 (s, 9 H, *t*-Bu), 3.7 (m, 2 H, CH_2), 3.97 (pseudo q, ^3J(H–P) $\simeq$ ^3J(H–H) = 7 Hz, 1 H, CHPh), 7.0–7.9 (m, Ph) (^{1}H NMR recorded at 200.13 MHz); ^{13}C NMR (C_6D_6) δ 27.66 (d, ^3J(C–P= 3.7 Hz, CH_3), 43.39 (d, ^1J(P–C) = 39.1 Hz, PCH_2), 52.54 (s, CMe_3), 55.41 (d, ^2J(C–P) = 10.0 Hz, *C*HPh), 197.34 (d, ^2J(C–P) = 7.4 Hz, cis CO), 199.03 (d, ^2J(C–P) = 25.9 Hz, trans CO); IR (decalin) ν(CO) 2075 (m), 1950 (sh), 1945 (vs) cm^{-1}; mass spectrum (^{184}W), *m/z* (relative intensity) 607 (M^+, 29), 579 (M^+ – CO, 15), 523 (M^+ – 3CO, 26), 467 (M^+–5CO, 100), 363 (WP(Ph)NC_4H_9, 87). Anal. Calcd for $C_{23}H_{22}NO_5PW$: C, 45.49; H, 3.65; N, 2.31; P, 5.10; W, 30.28. Found: C, 45.71; H, 3.45; N, 2.34; P, 5.15; W, 30.19.

Registry No. **1**, 82265-64-3; **2**, 82265-65-4; **3**, 82888-50-4; **4**, 82888-51-5; **5** isomer I, 88080-15-3; **5** isomer II, 88000-32-2; **6** isomer I, 109976-31-0; **6** isomer II, 110043-34-0; **9**, 109976-32-1; **10**, 88000-33-3; **11a**, 109976-33-2; **11b**, 109976-34-3; phenyloxirane, 96-09-3; *trans*-2,3-diphenylthiirane, 57694-36-7; 1-*tert*-butyl-2-phenylaziridine, 18366-49-9.

Reactions of $(\mu\text{-H})_3Fe_3(CO)_9(\mu_3\text{-}CCH_3)$. H_2 Displacement by CO and H_2 Elimination Following Deprotonation

Tamal K. Dutta, Xiangsheng Meng, Jose C. Vites, and Thomas P. Fehlner*

Department of Chemistry, University of Notre Dame, Notre Dame, Indiana 46556

Received March 26, 1987

The conversion of $(\mu\text{-H})_3Fe_3(CO)_9(\mu_3\text{-}CCH_3)$ (I) to $(\mu\text{-H})Fe_3(CO)_9(\mu\text{-CO})CCH_3$ (II) and the reverse reaction have been carried out via both direct and indirect routes. Direct H_2 displacement by CO and the reverse occur at 60 °C and 1–4 atm of pressure in an equilibrium process for which the equilibrium constant has been measured. The indirect route involves deprotonation of I in a reaction which is first order in I and first order in base. This is followed by a spontaneous, first-order cluster "oxidation" via H_2 elimination from an intermediate anion to yield $[(\mu\text{-H})Fe_3(CO)_9(CCH_2)]^-$ (III). Protonation of III followed by CO addition leads to II. On the other hand, protonation in the presence of H_2 at 1 atm of pressure leads to "reduction" of cluster III to I. These reactions are probed with isotopic labeling experiments that serve to define the mechanism for the indirect route relative to sites of deprotonation and dehydrogenation. Spectroscopic and kinetic evidence for the existence of intermediates in both processes is presented.

Although the metal cluster–metal surface analogy[1] has provided structural insight into the properties of organic fragments bound to multinuclear metal sites, it is perhaps most valuable in the area of chemical reactivity. Catalysts promote reactions, and, as has been pointed out in recent work,[2] stable structures need not be important species on a reaction pathway; i.e., characterized cluster complexes need not be relevant to a given reaction process. On the other hand, those aspects of a chemical reaction facilitated by interaction with more than a single metal atom will be important on surfaces as well as clusters. Hence, metal clusters provide a means of conveniently and clearly defining reactivity promoted by coordination to a multinuclear site.[3]

Due to the abundance of trinuclear systems that have been prepared and characterized,[4] reactions of organic fragments coordinated to the trimetal sites provided by these clusters constitute the most systematically studied systems.[5] For example, studies of the reactions of capped triosmium,[6,7] triruthenium,[8] triiron,[9–12] and mixed-metal

Chart I

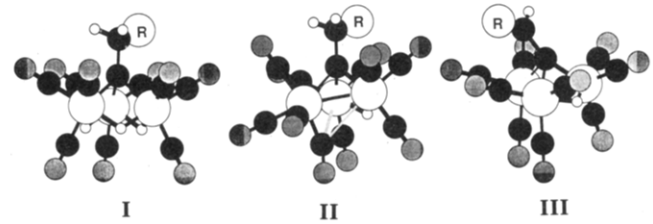

I II III

clusters[13,14] have already revealed considerable information on reaction type. These studies clearly demonstrate the ease of making and breaking metal and main-group element bonds to hydrogen on the clusters.[5] However, there is more to reactivity than product definition or even stoichiometry, and research reports on mechanistic aspects of cluster reactivity are appearing more frequently.[15–18]

(1) Muetterties, E. L.; Rhodin, T. N.; Band, E.; Brucker, C. F.; Pretzer, W. R. *Chem. Rev.* **1979**, *79*, 91.
(2) Beebe, T. P., Jr.; Yates, J. T., Jr. *J. Am. Chem. Soc.* **1986**, *108*, 663.
(3) Burch, R. R.; Muetterties, E. L.; Teller, R. G.; Williams, J. M. *J. Am. Chem. Soc.* **1982**, *104*, 4257.
(4) Wilkinson, G., Stone, F. G. A.; Abel, E. W., Eds. *Comprehensive Organometallic Chemistry*; Pergamon: New York, 1982.
(5) Deeming, A. J. In *Transition Metal Clusters*; Johnson, B. F. G., Ed.; Wiley: New York, 1980; p 391.
(6) See, for example: Shapley, J. R.; Cree-Uchiyama, M. E.; St. George, G. M. *J. Am. Chem. Soc.* **1983**, *105*, 140.
(7) Johnson, B. F. G.; Lewis, J. *Adv. Inorg. Chem. Radiochem.* **1981**, *24*, 225.
(8) See, for example: Bavaro, L. M.; Montangero, P.; Keister, J. B. *J. Am. Chem. Soc.* **1983**, *105*, 4977.
(9) See, for example: Kolis, J. W.; Holt, E. M.; Shriver, D. F. *J. Am. Chem. Soc.* **1983**, *105*, 7307.
(10) See, for example: Lourdichi, M.; Mathieu, R. *Organometallics* **1986**, *5*, 2067.
(11) See, for example: Andrews, M. A.; Kaesz, H. D. *J. Am. Chem. Soc.* **1979**, *101*, 7255.
(12) Wong, W.-K.; Chiu, K. W.; Wilkinson, G.; Galas, A. M. R.; Thornton-Pett, M.; Hursthouse, M. B. *J. Chem. Soc., Dalton Trans.* **1983**, 1557.
(13) Vahrenkamp, V. *Adv. Organomet. Chem.* **1983**, *22*, 169.
(14) Chetcuti, M.; Green, M.; Howard, J. A. K.; Jeffery, J. C.; Mills, R. M.; Pain, G. N.; Porter, S. J.; Stone, F. G. A.; Wilson, A. A.; Woodward, P. *J. Chem. Soc., Chem. Commun.* **1980**, 1057.
(15) Darensbourg, D. J. *Adv. Organomet. Chem.* **1982**, *21*, 113.
(16) Duggan, T. P.; Barnett, D. J.; Muscatella, M. J.; Keister, J. B. *J. Am. Chem. Soc.* **1986**, *108*, 6076.
(17) Brodie, N.; Poe, A.; Sekhar, V. J. *J. Chem. Soc., Chem. Commun.* **1985**, 1090.

0276-7333/87/2306-2191$01.50/0

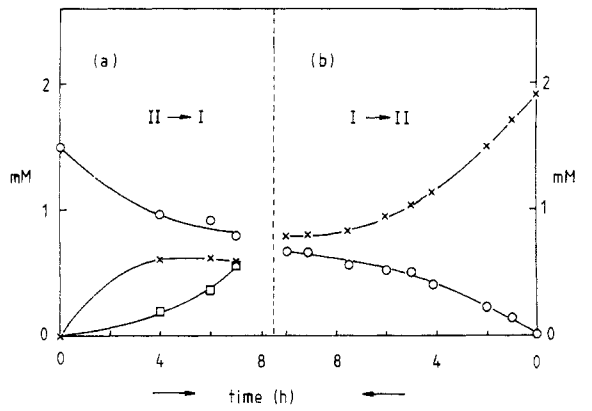

Figure 1. Approach to equilibrium for reaction 1 starting with pure II (a) and pure I (b): (○) II; (×) I; (□) $Fe(CO)_5$. The reaction was followed by infrared spectroscopy at 60 °C and 4 atm of pressure with $P(H_2)/P(CO) = 2.0$.

Likewise, in order to fully utilize these cluster systems as models for reactions on a surface, the manner in which an organic fragment is modified while bound to the cluster must be revealed. This requires detailed mechanistic information on reactions with clean stoichiometry.

Herein we present the results of a study of the ethyne-capped triiron system $(\mu\text{-H})_3Fe_3(CO)_9(\mu_3\text{-CCH}_3)$ (I, (Chart I), R = H) from the point of view of reactivity.[19] Both the structure and bonding of I have been analyzed previously via solid-state structural parameters, isoelectronic comparisons, photoelectron spectroscopic and quantum chemical analyses, and comparison with main-group model compounds.[20,21] Hence, in terms of the most stable structure, the reactant can be considered to be well understood, and these studies probe characteristics of less stable structures on the potential energy surface. Keister et al.[8,16] have reported several mechanistic investigations of the ruthenium analogue of I, and these studies are closely related to those reported here for the displacement of H_2 from I. However, light and heavy congeners do not always have the same geometric structures,[22] and, hence, reactivities may be substantially different as well. Thus, the two studies are complementary. We have also investigated the role of deprotonation/protonation in promoting reactivity of neutral/anionic hydridic clusters.[23] As will be seen, some reaction processes on the latter do not require elevated temperatures and the mechanistic results are more definitive.

CO Displacement of H_2 from I

Equilibrium. The reaction of I at 60 °C with 1 atm of CO under purge conditions for 5 h leads to the clean, partial (~40%) conversion of I to $(\mu\text{-H})Fe_3(CO)_9(\mu\text{-CO})(\mu_3\text{-CCH}_3)$ (II). When higher conversions are attempted or when the reaction is carried out in a closed system at higher pressures, e.g., 3–4 atm, fragmentation accompanies reaction 1 as evidenced by the production of

$$(\mu\text{-H})_3Fe_3(CO)_9(\mu_3\text{-CCH}_3) + CO \leftrightarrow (\mu\text{-H})Fe_3(CO)_9(\mu\text{-CO})(\mu_3\text{-CCH}_3) + H_2 \quad (1)$$

$Fe(CO)_5$. The reverse reaction (−1) occurs cleanly in a flow system at 1 atm of H_2; however, when a mixture of H_2/CO is used, fragmentation is also observed with the extent of fragmentation increasing with increasing relative amount of CO in the gas mixture. In separate experiments, we established that I is stable in the presence of excess H_2, but II reacts with CO to yield $Fe(CO)_5$ and other uncharacterized products. The lability of metal carbonyl clusters in general to degradation by CO is well-known[17,24] and, in this particular instance, complicates the investigation of the equilibrium behavior of (1). However, the following results, although not as precise as one might desire, do serve to define reaction 1 as one in which equilibrium can be established.

Figure 1 shows the composition of the system as determined by infrared spectroscopy as a function of time beginning with pure I or pure II and a H_2/CO ratio of 2. In the conversion of I to II, II accounts for 65% of I lost with no $Fe(CO)_5$ observable at 10 h. For the conversion of II to I, I accounts for 80% of II lost, but considerable fragmentation to produce $Fe(CO)_5$ occurs as early as 4 h into the reaction. Despite the presence of the fragmentation reaction and substantial systematic errors in the mass balance, it is clear that equilibrium for reaction 1 is being approached from both directions and that the two experiments bracket the equilibrium constant (Table I). The equilibrium constant at a single temperature was also determined from both directions by using ^1H NMR and a variety of H_2/CO ratios with the results shown in Table

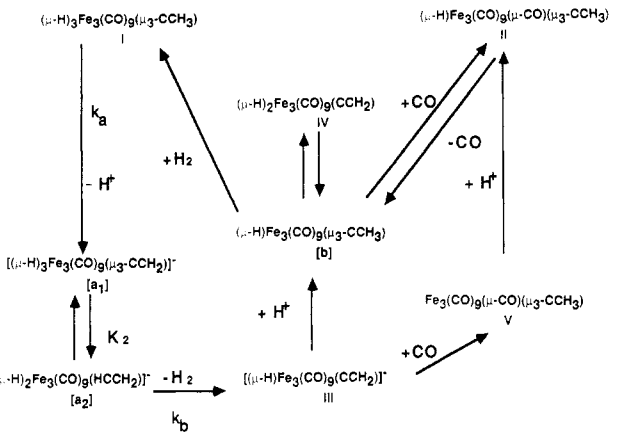

Figure 2. Comprehensive reaction scheme.

Table I. Equilibrium Constant Determinations for Reaction 1

$[II]_0/[I]_0$	t, h	$[II]/[I]$	$P(H_2)/P(CO)$	K_1[a]
0	7	1.45[b]	1.22[c]	1.75
0	7	2.44[d]	0.51[c]	1.25
∞	3	1.61[d]	1.35[c]	2.32
∞	5	0.50[d]	3.00[c]	1.52
0	10	0.85[e]	2.00[f]	1.70
∞	7	1.34[e]	2.00[f]	2.68

[a] Defined by reaction 1. See ref 19 for an error analysis. [b] 60 °C, 1-atm total pressure, C_6D_6 solvent; by integration of ^1H NMR CH_3 resonances of I and II. [c] By GLC analysis. [d] Same as *b* except 3-atm total pressure. [e] 60 °C, 4-atm total pressure, hexane solvent; by IR absorbances and extinction coefficients of I and II. [f] Commercial analyzed gas mixture.

(18) Hill, R. H.; Puddephatt, R. J. *J. Am. Chem. Soc.* **1983**, *105*, 5797.
(19) Vites, J.; Fehlner, T. P. *Organometallics* **1984**, *3*, 491.
(20) Wong, K. S.; Haller, K. J.; Dutta, T. K.; Chipman, D. M.; Fehlner, T. P. *Inorg. Chem.* **1982**, *21*, 3197. DeKock, R. L.; Wong, K. S.; Fehlner, T. P. *Ibid.* **1982**, *21*, 3203.
(21) The ruthenium and osmium analogues are known. Canty, A. J.; Johnson, B. F. G.; Lewis, J.; Norton, J. R. *J. Chem. Soc., Chem. Commun.* **1972**, 1331. Deeming, A. J.; Underhill, M. *J. Chem. Soc., Chem. Commun.* **1973**, 277. Yesinowski, J. P.; Bailey, D. *J. Organomet. Chem.* **1974**, *65*, C27.
(22) The two analogous compounds $M_3(CO)_{10}BH_3$ (M = Fe, Os) have different arrangements of the CO and H ligands. Vites, J. C.; Housecroft, C. E.; Jacobsen, G. B.; Fehlner, T. P. *Organometallics* **1984**, *3*, 1591. Shore, S. G.; Jan, D.-Y.; Hsu, L.-Y.; Hsu, W.-L. *J. Am. Chem. Soc.* **1983**, *105*, 5923.
(23) Dutta, T. K.; Vites, J. C.; Fehlner, T. P. *Organometallics* **1986**, *5*, 385.
(24) Lewis, J.; Johnson, B. F. G. *Pure Appl. Chem.* **1982**, *54*, 97.

Table II. ^1H and ^2H NMR Data for Isotopic Labeling Studies on Reactions 1, -1, and -2

reaction	I (^1H) δ 4.1[a]/ δ 23.6	I (^2H) δ 4.1[a]/ δ 23.6	selectivity, %	II (^1H) δ 4.1[a]/ δ 23.6	II (^2H) δ 4.1[a]/ δ 23.6
1. II + D_2[b] → I	1.43	0.62	62[c]		
2. V + D^+ → II				35/0	0/4
II + D_2[b] → I	2.52	0.61	62[c]		
3. III + D^+ → IV					
IV + CO → II			~80[d]		3.9[e]
4. III + D^+/H_2 → I	0.69	6.45	87[d]		
5. III + D^+ → IV					
IV + H_2[f] → I	0.78	5.44	84[d]		
6. III + H^+/D_2 → I[g]	3.29	0.065	94[c]		
7. III + H^+ → IV					
IV + D_2 → I	3.30	≤0.1	≥91[c]		

[a] ~90% R = CH_3. R = C_2H_5 and C_3H_7 included in ratio of integrals. [b] 60 °C at 1 atm. [c] For D in the FeHFe positions uncorrected for natural abundance of D. [d] For D in the CH_3 group uncorrected for natural abundance of D. [e] Ratio in unlabeled II is 16 in the ^1H NMR spectrum at 20 °C. [f] 30-min delay after acidification. [g] Spectra are illustrated in ref 23.

I. The two methods of determination give reasonable agreement and the average value of the equilibrium constant is 1.9. This value has not been corrected for the different solubilities of CO and H_2. The significance of the magnitude of the equilibrium constant with respect to the energetics of FeH vs. FeCO interactions has been presented earlier.[19] The experimental problems mentioned above precluded the determination of the equilibrium constant as a function of temperature. The value of the equilibrium constant for (1) is about the same as that previously measured for the ruthenium system. However, in the latter case, the substitutent on the quarternary carbon was CH_3O rather than CH_3.[8] For the ruthenium cluster, other substituents, X, on the capping carbon or different conditions lead to loss of CH_3X.[16,25]

Isotopic Labeling Studies. Reaction of I with ^{13}CO in a closed system led to the formation of II with all ten carbonyls enriched but not the quarternary or methyl carbons. The formation of $Fe(CO)_5$ was confirmed by the ^{13}C NMR experiments. Rate-limiting loss of H_2 has been observed in the ruthenium system studied earlier by Keister et al.[8,26] A similar mechanism, (2), is consistent with the observations presented thus far.

$$\text{I} \xrightarrow{\text{slow}} [Fe_3(CO)_9C_2H_4] + H_2$$

$$[Fe_3(CO)_9C_2H_4] + CO \xrightarrow{\text{fast}} \text{II} \qquad (2)$$

To probe the reverse reaction, particularly the regioselectivity of H_2 addition, the reaction of II with D_2 was examined. Examination of the product I with both ^1H and ^2H NMR (Table II,1) showed that while there was a small preference (~60:40) for iron over carbon sites, the D label was extensively scrambled throughout the FeH and CH positions. Second, the labeled cluster $(\mu\text{-}D)Fe_3(CO)_{10}(\mu_3\text{-}CCH_3)$ (II(D)) was prepared by treating the anion $[Fe_3(CO)_{10}(\mu_3\text{-}CCH_3)]^-$ (V) with D^+, and the label was shown to be in the FeHFe position by ^1H and ^2H NMR (Table II,2). II(D) was then heated in the presence of D_2 and the product I examined for deuterium content and location (Table II,2). The deuterium content of the FeH sites of I is about the same as that observed in the previous experiment, suggesting that the additional D is substantially randomized during the conversion of II to I. This is consistent with the mechanism 3 established for the

$$\text{II} \leftrightarrow [Fe_3(CO)_9C_2H_4] + CO \qquad (3a)$$

$$[Fe_3(CO)_9C_2H_4] + H_2 \xrightarrow{\text{slow}} \text{I} \qquad (3b)$$

ruthenium system by Keister et al.[7] Rapid scrambling of the D label in the unsaturated intermediate $[Fe_3(CO)_9C_2H_4]$, formed by reversible dissociation of CO from II, is suggested by our results. Because of the significant scrambling taking place on the time scale of the reaction, other possible labeling experiments were not carried out. It turned out to be more profitable to study reactions 1 and -1 carried out indirectly at reduced temperatures.

Deprotonation of I and Protonation of III

Anionic Route for CO Displacement of H_2 from I. A more convenient and higher yield conversion of I to II can be accomplished via reactions 4–6. Above 0 °C, de-

$$(\mu\text{-}H)_3Fe_3(CO)_9(\mu_3\text{-}CCH_3) + B: \rightarrow [(\mu\text{-}H)Fe_3(CO)_9CCH_2]^- + [BH]^+ + H_2 \qquad (4)$$

$$[(\mu\text{-}H)Fe_3(CO)_9CCH_2]^- + CO \rightarrow [Fe_3(CO)_9(\mu\text{-}CO)(\mu_3\text{-}CCH_3)]^- \qquad (5)$$

$$[Fe_3(CO)_9(\mu\text{-}CO)(\mu_3\text{-}CCH_3)]^- + H^+ \rightarrow (\mu\text{-}H)Fe_3(CO)_9(\mu\text{-}CO)(\mu_3\text{-}CCH_3) \qquad (6)$$

protonation of I leads to elimination of H_2 and the formation of the known[10,27] vinylidene anion $[(\mu\text{-}H)Fe_3(CO)_9CCH_2]^-$ (III) in 80% yield. Although a variety of bases, B:, have been investigated, stoichiometric addition of potassium acetate or addition of a trialkylamine are the most convenient methods. It has already been reported[10,27] (and reproduced here) that III reacts with CO at 25 °C to produce the anion of II, $[Fe_3(CO)_9(\mu\text{-}CO)(\mu_3\text{-}CCH_3)]^-$, (V) (reaction 5), which in turn is easily protonated to yield II (reaction 6). The reverse sequence of reactions can also be carried out. II is readily deprotonated with weak bases, and heating the anion under a purge of N_2 leads to III.[10,27] Protonation of III in the presence of 1 atm of CO leads to formation of II in quantitative yield while protonation in the presence of 1 atm of H_2 leads to a 70% yield of I with II being the major byproduct. In the following, a variety of experiments providing details of the mechanisms of reactions 4–6 are described.

Deuterium Labeling Studies. Clearly, in order to begin construction of a mechanism, the crucial information needed is knowledge of the sources of H^+ and H_2 in reaction 4 and the destinations in the reverse, i.e., of the two types of hydrogen in I, which supplies H^+ and which H_2? These questions are answered most directly by isotopic labeling provided label exchange in the products is slow relative to analysis time. As reaction -4 produces I which does not undergo H exchange rapidly, the conversion of III to I was examined first.

Two experiments were carried out. In one, III was treated with D^+ in the presence of H_2 while in the other III was treated with H^+ in the presence of D_2. The results of ^1H and ^2H NMR and mass spectrometric analyses are given in Tables II (4, 6) and III. For the first experiment, the ^2H NMR data show that 87% of the incoming deuterium ends up in the methyl group. With the assumption of 1:1 sensitivities for the CH and FeHFe resonances,[28] the combined ^1H and ^2H NMR data give a net deuterium

(25) Keister, J. B.; Payne, M. W.; Muscatella, M. J. *Organometallics* **1983**, *2*, 219.
(26) Dalton, D. M.; Barnett, D. J.; Duggan, T. P.; Keister, J. B.; Malik, P. T.; Modi, S. P.; Shaffer, M. R.; Smesko, S. A. *Organometallics* **1985**, *4*, 1854.
(27) Lourdichi, M.; Mathieu, R. *Nouv. J. Chim.* **1982**, *6*, 231.
(28) The actual ratio of integrals for unlabeled samples ranged from 1.08 to 1.41 depending on conditions.

Table III. Parent Ion Envelopes from the Mass Spectrum of $(\mu\text{-H})_3Fe_3(CO)_9(\mu_3\text{-}CCH_3)$ and Labeled Products

$Fe_3(CO)_9C_2H_6$ (I ref)		D^+/H_2 + III → I			H^+/D_2 + III → I		
	rel intensity		rel intensity			rel intensity	
m/e	obsd	m/e	obsd	calcd[a]	m/e	obsd	calcd[b]
451	26	453	7	4	453	29	26
450	100	452	41	37	452	100	100
449	13	451	100	101	451	14	13
448	26	450	78	78	450	29	26
447	3	449	43	29	449	7	3
446	13	448	15	18	448	7	13
		447	22	13			

[a] H_4D_2, 9%; H_5D, 60%; H_6 31%. [b] H_4D_2, 100%.

Table IV. ^1H NMR Analysis of the Protium Content of $[HN(C_2H_5)_3]^+$ from the Deprotonation of $I(D_2)$

	rel integral[a]		
compd	NH	CH_2	CH_3
$[HN(C_2H_5)_3]Cl$[b]	0.9 ± 0.1	6.0 ± 0.2	8.7 ± 0.3
$[HN(C_2H_5)_3]III$[c]	1.1	6.0	9.0
$[HN(C_2H_5)_3]III$[d]	1.1	6.0	11.2

[a] In $CDCl_3$ at 23 °C. [b] Four determinations over a concentration range of 0.1–0.3 M. [c] From I with normal isotopic abundances. [d] From $I(D_2)$.

content of 22% (17% expected for one D added). The mass spectrometric data (Table III) indicate a deuterium content of 13% and, although the D_1 species is most abundant, also show a significant amount of D_2 and D_0 species. The selectivity is high, and, despite evidence for some exchange, it seemed reasonable to conclude that protonation takes place predominantly at the C_2 fragment of III rather than at a metal–metal bond of the metal fragment.[23] However, as is made clear in the discussion below, the argument leading to this conclusion is not as straight forward as we first thought.[23]

The data in Table II (6) and III demonstrate that the H^+/D_2 experiment is a very clean one. The ^2H NMR spectra show that the deuterium enters the FeHFe positions with a selectivity of 94%. Taking into account the natural abundance of ^2H in III gives nearly quantitative selectivity. The ^1H and ^2H spectra together give a deuterium content of 40% (33% expected). Most importantly, the mass spectrum indicates a deuterium content of 33% showing the exclusive production of the D_2 species. The parent ion envelopes for the labeled and unlabeled compounds are identical within experimental error except the former is shifted up two mass units. High-resolution mass spectrometry showed the ratio of D_1:D_2:D_3 species to be 1:20:<1. Thus, the incoming H_2 goes selectively to the FeHFe positions of I, and, once formed, $(\mu\text{-H})(\mu\text{-D})_2Fe_3(CO)_9(\mu_3\text{-}CCH_3)$ ($I(D_2)$) does not undergo any scrambling reactions on the time scale of the experiment or on storage at 0–5 °C for 2 weeks.

The ability to prepare $I(D_2)$ allowed us to test (4) in the forward direction. With $N(C_2H_5)_3$ as the deprotonating agent, reaction 4 with $I(D_2)$ yielded only $[HN(C_2H_5)_3]^+$ by ^1H NMR (Table IV). This is a negative experiment and depends on the precise integration of a broad resonance. However, the experiment was carried out with both $[HN(C_2H_5)_3Cl$ and unlabeled $[HN(C_2H_5)_3]$ (III) as references, and the conclusion is consistent with the isotopic analysis of the dihydrogen produced on deprotonation (see below). Hence, deprotonation at the methyl group of $I(D_2)$ is indicated.

Analysis by mass spectrometry of the gases produced on deprotonation of $I(D_2)$ (Table V) showed D_2:HD:H_2 in

Table V. Mass Spectrometric Analysis of Dihydrogen from the Deprotonation of $I(D_2)$

	rel intensity	
m/e	run 1	run 2
4	0.46	0.40
3	0.46	0.46
2	0.08[a]	0.14

[a] This is a maximum value determined by variation of sample pressure in the source.

Table VI. Rate Coefficients for the Reaction of I with $N(C_2H_5)_3$[a]

$[I]_0$, mM	$[N(C_2H_5)_3]_0$, mM	k_{1st},[b] min^{-1}	k_{2nd},[b] M^{-1} s^{-1}
0.644	6.06	0.074 (0.993)	0.33 (0.977)
0.345	6.38	0.085 (0.997)	
0.355	6.90	0.098 (0.996)	
0.345	8.42	0.123 (0.998)	

[a] In hexane at 23 °C. [b] Correlation coefficients given in parentheses.

the ratio of 44:48:8; i.e., about 75% of the deuterium in $I(D_2)$ shows up as dihydrogen. As D_2 and HD are predominantly observed, dihydrogen elimination from $I(D_2)$ results from the FeHFe positions of the cluster. Statistical elimination of dihydrogen from $I(D_2)$ would result in a D_2:HD ratio of 1:2. The fact that the measured ratio is ~1:1 requires the presence of a substantial inverse kinetic isotope effect in the elimination process. The observed isotope effect for the thermal elimination of H_2 from $(\mu\text{-H})_3Ru_3(CO)_9(COCH_3)$ is normal (k_H/k_D = 1.4)[8,26] and similar to values observed in some mononuclear systems. Thus, a substantial difference in mechanism is indicated and is discussed below.

The fragmentation of $[HD_2Fe_3(CO)_9CCH_3]^+$ produced in a mass spectrometer by electron impact provides an interesting counterpoint supporting this interpretation. Three CO molecules are lost from the parent ion of $(\mu\text{-H})_3Fe_3(CO)_9(\mu_3\text{-}CCH_3)$ before H_2 loss becomes competitive with CO loss (branching ratio CO:H_2 = 1:4). Stripping the ion "cluster" corresponding to $[Fe_3(CO)_6C_2H_xD_y]^+$ shows loss of dihydrogen as D_2, HD, and H_2 in the ratio of 25:67:8. This shows preferred elimination of dihydrogen from the Fe_3 fragment and demonstrates the random elimination expected for a high-energy species.

These labeling studies suggest that protonation and deprotonation take place on the alkyl fragment and demonstrate that hydrogenation and dehydrogenation take place on the metal framework. Because of very different reaction conditions used in each case, they do not specify the order of protonation/deprotonation vs. hydrogenation/dehydrogenation. As spontaneous elimination of H_2 from I only takes place on heating to 60 °C or above for hours, deprotonation must precede H_2 elimination in going from I to III.[29] For the reverse reaction (–4) the situation is not as clear-cut. Hence, in the following we first explore some of the mechanistic characteristics of (4).

H_2 Elimination on Deprotonation of I: Mechanism of (4). The labeling results suggest several further mechanistic experiments. First, deprotonation at the CH_3 group of I should be subject to steric inhibition by large substituents replacing one or more hydrogens. To substantiate this point, the kinetics of reaction 4 for the

(29) Heating I under N_2 in C_6D_6 at 75 °C for 1 h resulted in 14% decomposition. With the assumption of a first-order reaction, this yields a rate constant of 8×10^{-5} s^{-1} which is a maximum value for the rate of H_2 elimination from I. The measured value for the anion a is 4×10^{-4} s^{-1} at 23 °C demonstrating a substantial reduction in activation energy for H_2 elimination on deprotonation of I.

Table VII. Variation in Alkyl Group Abundances During the Conversion of I to III and III to I

I		III[b]			I[d]		
R[a]	fractn	R′	fractn	rel rate[c]	R	fractn	rel rate[c]
CH_3	0.24	H	0.3	100	CH_3	0.56	100
C_2H_5	0.48	CH_3	0.38	26	C_2H_5	0.32	29
C_3H_7 C_4H_9	0.22 0.06	C_2H_5 $+C_3H_7$	0.24	30	C_3H_7 $+C_4H_9$	0.12	20

[a] See Chart I for definition of R and R′. [b] Produced from I with R distribution shown in column 1 via reaction 4 using CH_3COOK in $CH_3C(O)CH_3$ for 1 h at 23 °C. [c] Calculated on the basis of 90% conversion of I to III. [d] Produced from III with R distribution shown in column 2 via the reverse of reaction 2 with H_3PO_4/hexane for 20 min at 23 °C.

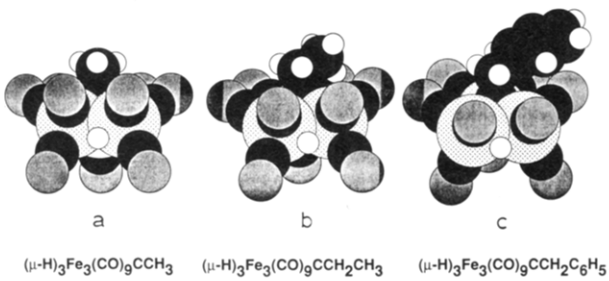

Figure 3. Representations of space-filling models of I: (a) R = H; (b) R = CH_3; (c) R = C_6H_5.

ethylidyne and benzylidyne derivatives (Figure 4) have been compared by using $N(C_2H_5)_3$ as the deprotonating agent. The reaction was carried out under pseudo-first-order conditions, and the loss of I was followed by infrared spectroscopy. The deprotonation of I is second order overall: first order in I and first order in base (Table VI). Under equivalent conditions the relative rate for the ethylidyne derivative is 9 times greater than that of the benzylidyne. As one might expect the protons on the $PhCH_2$ fragment to be more acidic than those on the CH_3 fragment, this rate reduction can only be due to the phenyl group hindering the attack of the base at the alkyl fragment of I. Note that part of the rate reduction on substituting phenyl for H in I is due to the decrease in the number of available protons from three to two on substitution of H by Ph.

In the preparation of I we obtain a mixture with R = H, CH_3, C_2H_5, etc. Early fractions from the protonation step (see Experimental Section) yield mainly R = H (~90%) while later fractions are enriched in the longer chain homologues. While conversions of I (R = H) to III are high, discrimination in conversion efficiencies is evident (Table VII) when I with a broader distribution of R groups is deprotonated with CH_3COOK. Under these conditions the base concentration is low and the overall rate similarly low. Hence, the relative conversion efficiencies provide a measure of relative rates of (4) as a function of R = C_nH_{n+3}. Under the conditions used the yield of III (R′ = H) is ~90%. This allows the relative rates shown in Table VII to be calculated. Although the magnitude of the difference in relative rates depends on the percent conversion used in the calculation, the order of reactivity does not. The substitution of H by CH_3 or C_2H_5 reduces the relative rate and the overall effect of an alkyl substituent is not that much different than that of C_6H_5. At first sight this is surprizing until one realizes (Figure 3) that the constraints of the C–C–phenyl torsional angle prevent the phenyl group from blocking the incoming base much more effectively than CH_3 or C_2H_5.

The volumetric measurement of the evolution of H_2 in reaction 4 provides another convenient measure of reaction progress. Rate measurements based on H_2 production were carried out by using $N(C_2H_5)_3$ as the deprotonating agent. The qualitative results are summarized in Figure 4 where the observed production of H_2 is compared with that calculated on the basis of the loss of I using the rate constant given in Table VI. Under these conditions it is obvious that the deprotonation process is separate from and more rapid than that of H_2 evolution. This demonstrates that the anion initially formed on deprotonation must have a significant lifetime and that the rate of H_2 evolution measures its unimolecular decay. In accord with this conclusion, plots of $\ln\{([H_2]_\infty - [H_2])/[H_2]_\infty\}$ vs. t are linear and yield the first-order rate constants given in Table VIII. Hence, the stoichiometric mechanism for (4) is

$$I + N(C_2H_5)_3 \xrightarrow{k_a} [a]^- \xrightarrow{k_b} III + H_2 \qquad (7)$$

where $[a]^-$ is an intermediate anion with the composition $[Fe_3(CO)_9C_2H_5]^-$ and $k_a = 0.33\ M^{-1}\ s^{-1}$ and $k_b = 4.3 \times 10^{-4}\ s^{-1}$ at 23 °C.

In an attempt to obtain structural information on the intermediate, we have followed the deprotonation of I by ^1H NMR. A half mole equivalent of $N(C_2H_5)_3$ was added to I in acetone-d_6 at −40 °C, and the NMR spectra were measured as the temperature was raised to 20 °C. A loss in intensity of the two resonances associated with I equal to the amount of amine added is accompanied by small, characteristic downfield shifts in the CH_2 and CH_3 resonances of $N(C_2H_5)_3$ as it is converted into $[HN(C_2H_5)_3]^+$. Deprotonation begins at 0 °C and is complete by the time 20 °C has been reached (Figure 5). However, although resonances corresponding to III appear, the rate of growth of this anion is much slower than the loss of I (Figure 5). In addition, the evolution of H_2 as measured by its ^1H NMR signal (δ 4.51 in acetone-d_6) parallels that of III. Again this requires the existence of an intermediate anion

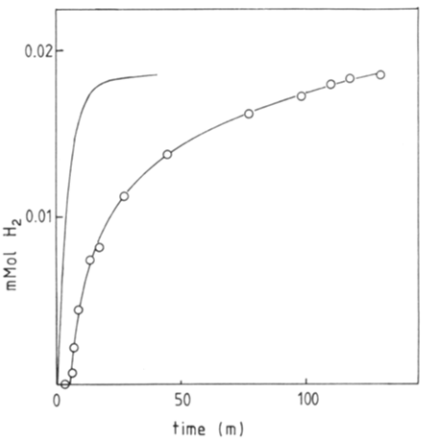

Figure 4. Plot of the evolution of H_2 as a function of time for reaction 4 in hexane at 24 °C with $N(C_2H_5)_3$ as the deprotonating agent. $[I]_0 = 2.8$ mM, and $[N(C_2H_5)_3]_0 = 14$ mM. The solid line without data points is the calculated H_2 production if 1 mol of H_2 is produced for each mole of I lost with no time delay. These calculations are based on a second-order reaction (first order in base and first order in I), the initial concentrations, and a rate constant of 0.33 $M^{-1}\ s^{-1}$.

Table VIII. Rate of H_2 Evolution in the Reaction of I with $N(C_2H_5)_3$[a]

$[H_2]_\infty$, mmol	$[I]_0$, mM	$[N(C_2H_5)_3]_0$, mM	$10^4\ k_{1st}$,[b] s^{-1}
0.018	4.5	>6	4.9 (0.993)[b]
0.019	2.8	14	4.7 (0.974)
0.042	6.4	28	3.2 (0.996)

[a] In hexane at 24 °C. [b] Correlation coefficients given parentheses.

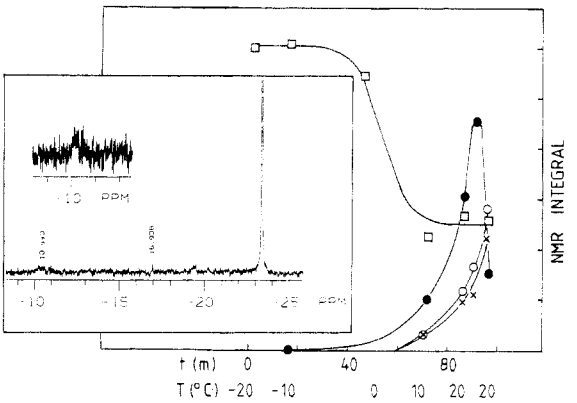

Figure 5. Reaction 4 (B: = $N(C_2H_5)_3$; in acetone-d_6) followed by ^1H NMR as a function of temperature: (□) I (δ −23.4 with intensity relative to solvent resonance); (×) III (δ 4.63 with intensity relative to I at δ 4.56). At 95 min the amount of III formed is 86% of the amount of I lost on the basis of NMR integrals; (○) H_2 (δ 4.53 with intensity relative to I at δ 4.56); (●) a_2 (approximate area of δ −10.4 in arbitrary units). The inset shows the spectrum in the high-field region at 90 min and 20 °C. Note that the hydride resonance of III at δ −16.9 integrates low with respect to the δ 4.63 resonance.

preceding the formation of III. During and immediately after deprotonation is complete, a weak, broad signal is observed at δ −10.4 with a time dependence characteristic of an intermediate (Figure 5). As the CHFe resonance of $[HFe_3(CO)_9(HCH)]^-$ appears at δ −10.1, we assign the δ −10.4 signal to intermediate a_2 in Figure 2. (The signal at δ −10.4 could also be due to a FeH hydride.) Small signals possibly due to the CH_2 and FeHFe signals required by a_2 are observed at δ 6.9 and −19.3; however, it is not possible to assign them unambiguously to a_2.[30] This spectroscopic evidence, combined with the information on the site of deprotonation, points to a mechanism involving intermediates a_1 and a_2 in Figure 2. Hence the formation of CHFe from FeHFe interactions prior to H_2 elimination is suggested.

Support for the proposed mechanism for the reductive elimination of H_2 from I can be derived from the kinetic isotope effect observed. The ratio of D_2/HD observed in the elimination of dihydrogen from I(D_2) (see above) requires a large inverse isotope effect ($k_H/k_D \approx 0.5$) for the conversion of I to III. In turn, this inverse isotope effect requires a preequilibrium involving an intermediate containing H in a position associated with higher stretching frequencies. Reasonable possibilities include FeH(terminal)[31] and FeHC(bridging). The latter is favored for two reasons. First, our work on the $Fe_3(CO)_9CH_4$ system,[32] in which the existence of three tautomeric forms involving replacement of FeHFe by FeHC interactions was demonstrated, shows that isomers of I involving CHFe interactions are energetically accessible. Second, studies of closely related ruthenium and osmium systems have revealed evidence for the formation and participation of MHC interactions in reactions involving hydrogen atoms.[16,30,33] Third, the NMR experiments described above provide direct evidence for such a species. Hence, we postulate a pathway involving an equilibrium between a_1 and a_2 as shown in Figure 2. This results in an estimated $K_{(2)H}/K_{(2)D} = 0.5$.[34] The H_2 elimination from a_2 will increase the overall calculated value somewhat, but agreement with the observed isotope effect is still acceptable.

H_2 Addition on the Protonation of III: Mechanism of (−4). Three routes for the conversion of III to I (Figure 2) are reasonable. One is the reverse of the path whereby III is formed from I. The second is direct formation of IV followed by hydrogenation, and the last is hydrogenation of IV via intermediate b which is a tautomer of IV (Figure 2).[35] The experimental conditions mitigate against a path via $[a]^-$ as the solid salt of III is treated with H_3PO_4/hexane in the prescence of H_2. An efficient gas–solid reaction under these conditions seems unlikely although not impossible. In addition, treatment of III in acetone solution with H_2 at 1 atm of pressure for ca. 1 h did not result in the significant loss of III by NMR. Hence, we are left with the problem of distinguishing two pathways that are only subtly different.

Before this question can be discussed, it is necessary to discuss the site of protonation of III. We sought direct evidence for the site of protonation by protonating the $[Et_3NH^+]$ salt of III in CD_2Cl_2 with CF_3COOH at −60 °C while the reaction was observed by ^1H NMR. The only major product observed under these conditions is $(\mu\text{-}H)_2Fe_3(CO)_9CCH_2$ (IV). Thus, if protonation takes place at the hydrocarbyl fragment of III, hydrogen rearrangement must be very rapid. However, weak broad signals at δ −8.7 and −23.0 in an intensity ratio of 1:1 were also observed. We attribute these to a tautomer of IV, $(\mu\text{-}H)Fe_3(CO)_9(HCCH_2)$, which is analogous to $[a_2]$. This species may or may not be involved in the hydrogenation pathway.

Additional evidence concerning the site of protonation comes from the observation of a steric effect on reaction −4. If protonation takes place at the vinylidene fragment of III, substitution at the β-carbon should retard the reaction rate in a manner analogous to that observed for I → III. Table VII contains the initial distribution of alkyl groups on III as determined by ^1H NMR as well as the distribution of alkyl on I produced from it (third column). Conversion efficiency falls off as the size of the alkyl group increases, and, with the assumption of a 90% conversion of R′ = H, the relative rates shown can be calculated. The decrease in rate with alkyl substitution is consistent with protonation at the alkyl fragment of III but does not

(30) Such a species has been implicated in the reactions of the ruthenium analogue of I. See ref 16 and: Bower, D. K.; Keister, J. B. *J. Organomet. Chem.* **1986**, *312*, C33.

(31) In this explanation H_2 elimination from the initially formed anion (a_1) involves the conversion of two FeHFe hydrogens into two FeH(terminal) hydrogens. As the zero-point energy is lower for FeH(bridge) than for FeH(terminal), the lighter isotope will prefer the bridging position. This equilibrium isotope effect, however, cannot account for more than a factor of 1.2 favoring D_2 elimination in the overall reaction ($K_H/K_D \approx 0.8$). However, an inverse isotope effect ($k_H/k_D = 0.72$) has been observed for H_2 elimination from a mononuclear platinum compound and is interpreted in terms of a late transition state. Packett, D. L.; Trogler, W. C. *J. Am. Chem. Soc.* **1986**, *108*, 5036. Hence, if the formation of corrdinated H_2 is rate-limiting for reaction 4, there would be an additional contribution to the observed inverse isotope effect. Although FeH bonds are being broken (~2000 cm^{-1}), a strong HH bond is being formed (4280 cm^{-1}) in a later transition state. Reasonable estimates of the frequency changes lead to an estimate of $k_H/k_D \approx 0.6$, and, hence, an overall isotope effect of $k_H/k_D \approx 0.5$. Intramolecular displacement of the H_2 ligand completes the reaction. This explanation, although possible, suffers from the difficulty of envisioning a reasonable structure for a closed M_3C cluster with nine CO and two terminal H ligands.

(32) Vites, J. C.; Jacobsen, G.; Dutta, T. K.; Fehlner, T. P. *J. Am. Chem. Soc.* **1985**, *107*, 5563. Dutta, T. K.; Vites, J. C.; Jacobsen, G. B.; Fehlner, T. P. *Organometallics* **1987**, *6*, 842.

(33) VanderVelde, D. G.; Shapley, J. R. *Abstr. Pap.—Am. Chem. Soc.* **1984**, *187th*, INORG 129.

(34) $K_{(2)H}/K_{(2)D} \approx \exp(0.146)(1.44)(2600 - 1600)/T$ [Benson, S. W. *Thermochemical Kinetics*; Wiley: New York, 1968] where 2600 and 1600 cm^{-1} are the estimated stretching frequencies of the CHFe and FeHFe hydrogens, respectively [Cooper, C. B., III; Shriver, D. F.; Onaka, S. *Adv. Chem. Ser.* **1978**, *No. 167*, 232].

(35) The Ru and Os analogues of IV hydrogenate to the analogues of I. Eady, C. R.; Johnson, B. F. G.; Lewis, J. *J. Chem. Soc., Dalton Trans.* **1977**, 477. Deeming, A. J.; Underhill, M. *J. Chem. Soc., Chem. Commun.* **1973**, 277.

eliminate an explanation based on slower H_2 addition with increasing alkyl group size.

The relative sensitivities of the CCH_3 and FeHFe ^1H NMR resonances to different solvents provides circumstantial evidence for deprotonation at the alkyl fragment. For example, in acetone the CCH_3 resonance shifts 0.4 ppm downfield while the FeHFe resonance shifts 0.2 ppm in the same direction. This suggests that the former site interacts more strongly with the solvent and is more accessible to attack by a base.

The acidification experiments with D^+ provide information pertinent to the question of whether the conversion of III to I or II proceeds through intermediate b or IV or both. Although 80–90% selectivity was observed in the D^+/H_2 + III experiment under conditions that optimized the yield of I, some scrambling of the label was evident. To investigate this point in more detail, a delay time was introduced between acidification and hydrogenation. This reduced the yield of I and increased that of II (total yield decreasing). At the same time the selectivity remained the same within experimental error (see Table II, 5, for 30-min delay). Proton spectra showed little additional loss of selectivity with delay times of several hours. The ^1H NMR of IV formed from III and D^+ taken after ca. 1 h suggests $\leq$65% enrichment of the CCH_2 position with deuterium. Thus, if protonation takes place at either the alkyl group or the metal–metal bond, the deuterium label is substantially randomized in the formation of IV. However, hydrogenation of the same sample of IV in the absence of acid still leads to high deuterium content in the CCH_3 group of I (Table II, 5).[34] Thus, the selectivity observed in the D^+/H_2 experiment cannot be due to selective protonation at the alkyl fragment of III. In addition, carbonylation of IV(D) produces II with a high deuterium content in the CCH_3 fragment (Table II, 3). The riddle posed by these observations is explained with the following mechanism.

If IV and b are in equilibrium as indicated in reaction 8, then as the conversion of IV to b involves the transfer of a FeHFe hydrogen to a CH terminal site, the distribution of D between IV and b is governed by an equilibrium isotope effect favoring D in the site with the strongest bond, i.e., CH. In addition, there is a statistical factor

$$\underset{\text{IV}}{H_2Fe_3(CO)_9CCH_2} \leftrightarrow \underset{\text{b}}{HFe_3(CO)_9CCH_3} \qquad (8)$$

favoring D in the CH sites of b. For the purposes of this argument consider only two types of sites on b, namely, CH and FeHFe with frequencies of 3100 and 1600 cm^{-1}. The calculated equilibrium fractionation factor is 2.9 favoring CD over FeDFe site occupancy in b, and the statistical factor is 3 in the same direction, i.e., a combined selectivity of 90% for the CCH_2 fragment.[36] Hence, the indirect mechanism (9) provides a logical explanation of

$$\text{III} + H^+ \rightarrow [\text{b}] \leftrightarrow \text{IV}$$
$$[\text{b}] + H_2/CO \rightarrow \text{I/II} \qquad (9)$$

why total scrambling of the label still leads to a preference for D in the alkyl fragment that has nothing to do with the original site of protonation. On the other hand, the equilibrium enrichment calculated for IV[37] is not high enough to account for that observed in I or II. Therefore, a direct reaction of IV with H_2 or CO that preserves the label distribution is eliminated. Note that the tautomer of IV may be involved in the formation of b without changing the argument.

Support for this conclusion comes from an experiment in which the cycle I to III to I was carried out twice by using H^+/D_2. As the reaction with D_2 is clearly regiospecific, the label distribution in the product after two cycles provides information on the label distribution in III after one cycle. The ^1H and ^2H NMR intensity data allow the deuterium content as well as distribution between basal and apical sites to be determined. After two cycles I contains 3.2 D atoms with 75% D in the iron sites and 25% in the hydrocarbon sites. This means that the precursor vinylidene III must have had 1.2 D atoms with 33% and 67% D in iron and hydrocarbon sites, respectively. This is consistent with total scrambling in III in less than $^1/_2$ h with deuterium fractionation in the direction expected. Indeed if one uses the equilibrium fractionation observed here for III as a measure of that expected for (8), then the calculated enrichment in the alkyl fragment of b is 86% as observed (Table II, 4 and 5).

Finally, we must consider the reaction of b with H_2 and CO. As b is formally unsaturated, one might expect these two reactions to be competitive. However, even under a vigorous H_2 gas purge, traces of CO produce II as the major byproduct in the formation of I from III. Thus, the apparent reactivity of b with CO must be much larger than that with H_2. A similar situation arises for the thermal reaction of the ruthenium analogue.[26]

The facile reaction of III with CO[27] may well proceed through an unsaturated intermediate analogous to b.[38] If so, one might expect clean addition of other Lewis bases leading to the indirect substitution of II. Addition of $PPh(CH_3)_2$ to III in acetone followed by protonation produced a mixture of II and a single substitutional isomer of $(\mu\text{-}H)Fe_3(CO)_9(PPhMe_2)(\mu_3\text{-}CCH_3)$ (II′) with the latter compound in higher yield. The lack of P–H coupling to the hydride suggests phosphine substitution on the unique iron atom of II. This is consistent with stabilization of the vacant coordination site of III or IV by the vinylidene double bond.[26] Direct substitution of II with $PPh(CH_3)_2$ was not observed on the same time scale. Hence, both III and IV can be viewed as ready precursors of unsaturated sites on the metal framework.

Conclusions

A summary of the experimental observations are given by the mechanism presented in Figure 2. The significance of this work exceeds the bare mechanistic facts. First, the generation of a site of Lewis basicity on a hydrocarbyl ligand (vinylidene) on a cluster system promotes the elimination of dihydrogen. This is consistent with our independent studies of phosphine substitution on the analogous ferraboranes[39] as well as the work of Keister et al.[25,26] Second, note that the production of a_1 from I and b from III constitutes the nonthermal generation of intermediates. Therefore, kinetically controlled deprotonation of hydridic compounds and protonation of anions constitutes one method of entering neutral cluster reaction surfaces at nonequilibrium structures and energies.[32] Protonation/deprotonation is as an effective modifier of the reactivity of clusters as it is of classical coordination complexes.[40] Third, these cluster reactions appear to take

(36) This ignores any isotope effect in the conversion of b to I or II.
(37) Note that IV should have a similar equilibrium fractionation of D favoring the alkyl fragment if an equilibrium distribution is achieved.
(38) The reaction of CO with III has been reported to be much slower for larger substitutents than H on the methyl carbon. Mathieu, R.; Suades, J. *J. Organomet. Chem.* **1986**, *312*, 335.
(39) Housecroft, C. E.; Fehlner, T. P. *J. Am. Chem. Soc.* **1986**, *108*, 4867.
(40) Wilkins, R. G. *The Study of Kinetics and Mechanism of Reactions of Transition Metal Complexes*; Allyn and Bacon: Boston, 1974.

Table IX. ^{1}H NMR Spectra[a] for $(\mu\text{-}H_3)Fe_3(CO)_9(\mu_3\text{-}CCH_2R)$ (I), $(\mu\text{-}H)Fe_3(CO)_9(\mu\text{-}CO)(CCH_2R)$ (II), $[(\mu\text{-}H)Fe_3(CO)_9(CCHR')][HN(C_2H_5)_3]$ (III), and $(\mu\text{-}H)_2Fe_3(CO)_9(\mu_3\text{-}CCHR')$ (IV)

compd (R)	CH_2R	FeHFe[b]
I (H)	4.10 (q[b])	−23.57 (q)
I (CH_3)[c]	4.37 (q, CH_2), 1.5. (t, CH_3)	−23.59 (t)
I (C_2H_5)[c]	4.52 (t, CH_2), 2.17 (m, CH_2), 0.97 (t, CH_3)	−23.54 (t)
I (C_3H_7)[c]	4.58 (t, CH_2), 2.19 (m, CH_2), 1.49 (m, CH_2), 0.91 (t, CH_3)	−23.51 (t)
I (C_6H_5)	7.7–7.4 (m, C_6H_5), 4.95 (s, CH_2)	−23.4
II (H)	3.95 (d[b])	−19.93
II (CH_3)[c]	4.18 (q, CH_2), 1.43 (t, CH_3)	−20.40
II (C_2H_5)	4.30 (t, CH_2), 2.01 (m, CH_2), 0.91 (t, CH_3)	−19.78
III (H)[d]	4.63 (d,[e] CH_2)	−16.99
III (CH_3)	5.59 (m, CH), 1.28 (m, CH_3)	−17.31
III (C_6H_5)	7.7–7.3 (m, C_6H_5), 5.34 (s, CH_2)	−16.3
IV (H)	4.45	−19.4
		−26.4

[a] I, II, IV (C_6D_6, 20 °C); III ($CD_3C(O)CD_3$, 20 °C). Chemical shifts in δ. [b] Coupling between FeHFe and the $-CH_2$ group ≈ 1.2 Hz when observed. [c] Vicinal coupling constant ≈ 6 Hz. [d] $[HN(C_2H_5)_3]^+$ salt: δ 4.0 (br), 3.45 (q, J = 7 Hz), 1.40 (t, J = 7 Hz). [e] Coupling constant ≈ 2 Hz.

place via complex, competitive and consecutive reaction pathways involving a number of intermediates that do not differ greatly in energy. As a consequence, low reaction temperatures are required to maximize mechanistically significant information from a given system.[41]

In a real sense, the mechanistic complexity observed here reinforces the metal cluster–metal surface analogy.[1] For example, recent studies of surface bound alkylidyne fragments have revealed mechanistic aspects closely related to those exhibited by the discrete systems discussed here.[42,43] One of these investigations presents evidence supporting a mechanism for the exchange of deuterium with the CCH_3 fragment on Pt(111) that involves a unimolecular isomerization preceding the isotopic exchange step.[43] The isomer produced, and the active species in the exchange, was postulated to be a vinyl fragment, and, hence, the proposed isomerization bears a close similarity to the isomerizations a_1 to a_2 and IV to b given in Figure 2. Indeed evidence was presented above for an isomer of IV containing a vinyl moiety. It may well be that the interconversions observed in the discrete system also constitute reaction pathways for the interconversion of the same hydrocarbyl fragments on metal surfaces.

Experimental Section

General Data. All reactions and manipulations were carried out under inert atmospheres or in a vacuum line with standard techniques.[44] Solvents were dried (THF over KOH pellets, hexane and toluene over molecular sieve), degassed, and distilled before use; methanol and dichloromethane were dried over molecular sieve and degassed before use. $Fe(CO)_5$ (Alfa) and acetyl chloride (Fisher) were fractionated in a vacuum line, BH_3·THF (1 M, Aldrich) was titrated, and H_3PO_4 (85%) (Fisher) was degassed before use. The following were used as received: $KC_2H_3O_2$ (Coleman & Bell), $NaHCO_3$ (Fisher), $N(C_2H_5)_3$ (Eastman), C_6H_5CCH, (Aldrich), $NaFe(CO)_4$·1.5($C_4H_8O_2$) (Alfa and Aldrich), CF_3COOH (Aldrich), $(CH_3)_2(C_6H_5)P$ (Aldrich), and [PPN]Cl [bis(triphenylphosphine)nitrogen(1+) chloride] (Aldrich). Hydrogen, deuterium, carbon monoxide, and a preanalyzed mixture of H_2 and CO (Union Carbide, Linde) were used as received. Column chromatography was performed on 60–200 mesh silica gel (Baker) or acidified silica gel (treatment with 1.5 M H_3PO_4 in methanol followed by drying at 100 °C overnight). Centrifugal thin-layer chromatography employed silica gel and acidified silica gel plates.[45]

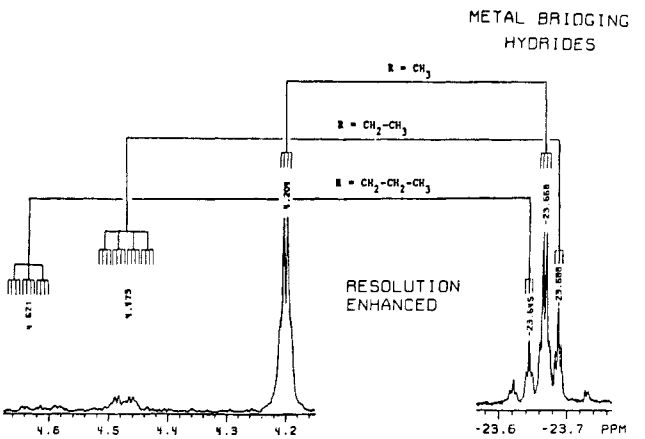

Figure 6. Resolution-enhanced ^{1}H NMR spectrum of I showing the coupling of the FeHFe and alkyl protons.

^{13}C, ^{31}P, ^{2}H, and ^{1}H FT NMR spectra were obtained on a Nicolet 300-MHz spectrometer. Some ^{1}H NMR were obtained on a Chemagnetics 200-MHz spectrometer. ^{13}C shifts are reported with respect to residual solvent signals (toluene-d_8, δ 137.5, and benzene-d_6, δ 128.0), ^{31}P shifts with respect to H_3PO_4 external standard (δ 0), ^{2}H with respect to internal benzene-d_6 (trace), and ^{1}H shifts with respect to residual solvent signals (benzene-d_6, δ 7.15, and acetone-d_6, δ 2.04). General infrared spectra were recorded on a Perkin-Elmer 983 spectrometer, and quantitative IR analyses were carried out with an IBM Model IR32 FT-IR using 0.2-mm CaF_2 solution cells. The Beer's law plots for I, II, and $Fe(CO)_5$ were based on bands at 2062, 2044, and 2020 cm^{-1}, respectively. Mass spectra were run on a AEI-MS 9 spectrometer. A Carle Model 311 gas chromatograph with molecular sieve and POROPAK columns in series and argon carrier gas was used to qualitatively identify H_2, CO, and CH_4. Authentic gas samples were used for calibration.

Preparation and Characterization of I, II, and III. $(\mu\text{-}H)_3Fe_3(CO)_9(\mu_3\text{-}CCH_3)$ (I). The alkyl derivatives were prepared by the reduction of acetyltetracarbonylferrate(0) salts by BH_3·THF under the following conditions. The $[(CO)_4FeC(O)CH_3]^-$ sodium salt was prepared according to reported procedures.[46] The salt was used directly from THF solution after solids were removed by filtration. In a typical preparation 4 mmol of $Fe(CO)_5$ were mixed with 2 mmol of $[(CO)_4FeC(O)CH_3]Na$ dissolved in 20 mL of THF. Four millimoles of 1 M BH_3·THF was then added with stirring at 23 °C. Gas evolution was observed as the solution turned deep red. After 1 h the solvent and unreacted $Fe(CO)_5$

(41) Deeming has studied the reaction of D_2 with the osmium analogue of IV and reported evidence supporting preferential deuteriation of the alkyl moiety of the osmium analogue of I which is formed.[35] As the reaction requires heating for long periods of time, it is quite possible that he was observing the equilibrium distribution of D in I.[37] If so, these observations have no significance relative to the mechanism of H_2 addition to IV.

(42) Koel, B. E.; Bent, B. E.; Somorjai, *Surf. Sci.* **1984**, *146*, 211.

(43) Ogle, K. M.; White, J. M. *Surf. Sci.* **1986**, *165*, 234.

(44) Shriver, D. F. *Manipulation of Air Sensitive Compounds*; McGraw-Hill: New York, 1975.

(45) Stahl, E. *Angew. Chem., Int. Ed. Engl.* **1983**, *22*, 507.

(46) Alper, H.; Tanaka, M. *J. Am. Chem. Soc.* **1979**, *101*, 4245.

were removed under vacuum. The remaining viscous red oil was treated with 10 mL of degassed H_3PO_4 and 10 mL of hexane resulting in vigorous gas evolution. The neutral products were extracted into the hydrocarbon phase with vigorous shaking or sonication to maximize acidification of the red oil. The organic phase contained I as well as other products. Further material could be obtained by additional extractions.

The products contained in the hexane solution were separated by normal column chromatography or centrifugal thin-layer chromatography with hexane as an eluent. I elutes as a yellow-orange band (R_f 0.5) which, on removal of solvent, forms a brown solid. In this procedure, I is obtained as a mixture of several homologues, $(\mu\text{-}H)Fe_3(CO)_9(\mu_3\text{-}CCH_2R)$ differing only in the alkyl chain length of R. The $^1H\{$select $^1H\}$ NMR spectra (Table IX) show that the alkyl chains are linear. This is particularly clear in the resolved proton–proton coupling between the hydrogens on the β-carbon of I and the FeHFe protons, e.g., Figure 6. The alkyl chain length distribution observed depended on the number and length of time of the extractions during acidification. For relatively short acidification times, R = H constituted ~90% of the sample. Yields based on 10 mmol of the acetyl salt ranged from 0.04 to 0.1 g of I for short and long acidification times, respectively. I: MS, p^+ 449.806 measd, 449.805 calcd, loss of nine CO's observed; IR (hexane, cm^{-1}): 2059 (vs), 2020 (vs), 2002 (m); ^{13}C NMR ($C_6D_5CD_3$, −100 to 20 °C) δ 270.9 (s, $C\text{-}CH_3$, J_{CC} = 33 Hz), 206.0 (s, 9 CO), 45.6 (s, CCH_3, J_{CC} = 33 Hz).

$(\mu\text{-}H)_3Fe_3(CO)_9(\mu_3\text{-}CCH_2C_6H_5)$ (I′). I′ was prepared in the same manner as I except that $Na[Fe(CO)_4C(O)C_6H_5]$ was used as the starting material. Reaction products included I as well as I′, indicating cleavage of the acyl group during the course of this complex reaction. Separation was by repeated centrifugal chromatography with hexane. I′ appears as an orange band immediately following the green $Fe_3(CO)_{12}$ band (R_f 0.35). The ^1H NMR parameters are given in Table IX. I′: MS, p^+ 526, loss of nine CO's observed; IR (hexane, cm^{-1}) 2061 (vs), 2022 (vs), 2003 (m).

$(\mu\text{-}H)Fe_3(CO)_9(\mu\text{-}CO)(CCH_3)$ (II). This compound was initially obtained from the same procedure as described for I. It appears as a dark red band in the chromatography (R_f 0.45) procedure. Yields were approximately the same as for I, and again R = CH_3, C_2H_5, etc. were observed with similar distributions. The ^1H NMR are given in Table IX. II: MS, p^+ 475.785 measd, 475.785 calcd, loss of 10 CO's observed; IR (hexane, cm^{-1}) 2095 (w), 2052 (s), 2042 (s), 2018 (s), 2000 (m, sh), 1998 (w), 1887 (w, br).

Alternatively, II can be prepared directly from I as described in the main body of the text. A better preparation has been reported by Mathieu et al.,[10] and, in fact, the spectroscopic properties of this compound have been reported twice while these studies were in progress.[12,27] However, as there are a number of inconsistencies between our data and those that were presented earlier and as no one has reported a solid-state structure, our data with a complete analysis are presented here.

In the proton NMR the FeHFe resonance is broad at 23 °C but sharpens at −40 °C and integrates to 1 H relative to the methyl resonance. The latter is a doublet with a 1.2-Hz coupling constant confirming the presence of a single FeHFe hydrogen. At 23 °C the ^{13}C NMR spectrum exhibits a broad quarternary carbon resonance at δ 310.8, a single carbonyl resonance at δ 209.6, and a methyl carbon resonance at δ 46.2. As the temperature is lowered, the resonance at δ 310.8 sharpens and the carbonyl resonance begins to "freeze" out. At −50 °C three resonances of approximate equal intensity are observed at δ 206.3, 207.0, and 208.7 and are assigned to the six CO's on the two equivalent iron atoms in the structure in Chart I. In this temperature range (−50 to −60 °C) a broad resonance at δ 213 is also observed and assigned to the four CO's on the unique iron atom. At −90 °C the broad δ 213 signal has disappeared and additional signals at δ 224.1 and 210.5 in an intensity ratio of 1:2 have appeared (Figure 7). There is still one CO resonance missing. From the observed δ 224.1 and 210.5 resonances corresponding to three CO's and the average resonance of the four CO's at −60 °C, the calculated chemical shift of the missing CO is 207; i.e., the missing CO is hidden under the δ 207 peak due to two CO's on the other two iron atoms. In summary, the ^{13}C NMR shows that the molecule possesses a plane of symmetry. In addition, the carbonyl resonance at 224 ppm

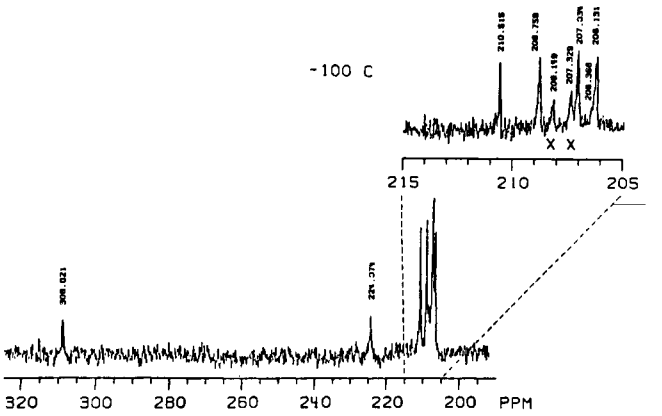

Figure 7. ^{13}C NMR of ^{13}C-enriched II at −100 °C. The resonances marked with an (×) are assigned to the ethylidyne derivative.

is not downfield enough to be a fully bridging carbonyl, and, hence, a semibridging carbonyl is proposed. This is consistent with the weak, broad peak at 1887 cm^{-1} observed in the infrared. These observations are summarized in the structure in Chart I.

The observed ^{13}C NMR behavior of II is similar to that observed in the related crystallographically characterized systems $[HFe_3(CO)_{10}(\mu\text{-}CO)]^-$ and $HFe_3(CO)_{10}(\mu\text{-}COCH_3)$.[47-48] A comparison of the ^{13}C NMR chemical shifts allows some further structural details of II to be deduced. For both of the model compounds, the low-temperature-limiting spectra show a set of seven resonances in the order and ratio 1:1:1:2:2:2:2. The first is the edge bridging carbonyl, and it is shifted 70 ppm downfield from the rest of the CO peaks. The other two low-field resonances of unit intensity are due to the inequivalent axial carbonyls on the unique iron atom. In II, one of these resonances (δ 224) is in the same range as the model compounds (δ 222, 221:δ 214, 213) whereas the other is at higher field (calculated at δ 207). This upfield shift is attributed to a steric interaction of the capping CCH_3 fragment with the axial carbonyl on the same side of the Fe_3 triangle. Precedence for this interpretation is given by the ^{13}C NMR of $HOs_3(CO)_{10}CH$.[49] Hence, the structure proposed for II contains a semi-triply bridging CO and an unsymmetrical triply bridging CCH_3 fragment as shown in Chart I.

Our ^1H NMR data agree well with those presented by Mathieu et al.[10,27] but differ significantly from those reported by Wilkinson et al.[12] On the other hand, the ^{13}C data do not agree completely with either of the previous studies. Our observations provide an explanation of the data reported earlier. Wilkinson et al. report a FeHFe resonance at δ −23.78 for II, the value we observe for I.[12] Noting that the FeHFe resonance is broad and weak for II at 23 °C and the CH_3 and FeHFe signals of I appear in a 1:1 ratio, we suggest that their sample was a mixture of II and I. In the CO region of the ^{13}C NMR spectrum (apparently at room temperature) Wilkinson et al. report four signals at δ 210.2, 209.2, 206.1, and 205.6 rather than the single one we observe. The first could be due to $Fe(CO)_5$, the second to II, and the fourth to I, and the third is unknown. Again a mixture is suggested. On the other hand, Mathieu et al. report a single CO resonance at room temperature (δ 209.7) as do we and three at −90 °C (δ 207.8, 206.3, 205.3) in the ratio of 4:3:3.[10] As the latter three resonances correspond well with the three pairs of CO's we observe as sharp resonances at −60 °C and as the three do not average to the chemical shift of the single room-temperature resonance, we suggest Mathieu et al. did not achieve the low-temperature-limiting spectrum reported here. However, the structure proposed by Mathieu et al. is identical with the one we suggest.

Equilibrium Studies. Infrared and ^1H NMR spectroscopies were used for the equilibrium studies. In the former, Beer's law plots were prepared separately for I, II, and $Fe(CO)_5$ covering the concentration range of the studies. A constant H_2/CO ratio and temperature were employed (2:1, 60 °C). Reactions were carried

(47) Wilkinson, J. R.; Todd, L. J. *J. Organomet. Chem.* **1976**, *118*, 199.
(48) Shriver, D. F.; Hadali, H. A. *Inorg. Chem.* **1979**, *18*, 1236.
(49) Shapley, J. R.; Cree-Uchiyama, M. E.; St. George, G. M.; Churchill, M. R.; Bueno, C. *J. Am. Chem. Soc.* **1983**, *105*, 140.

out in a pressure bottle at 4-atm total pressure with hexane as solvent. Samples were withdrawn periodically for IR analysis. Figure 1 shows composition as a function of time for both reactions. The NMR experiments were carried out in the same apparatus with essentially the same procedures. Integrals of the ^1H methyl resonances of I and II were used as measures of the relative concentrations of each. For the NMR studies, gas composition was varied and the gas mixture was analyzed by gas chromatography using peak areas with sensitivities obtained by calibration with pure gas samples. A summary of the results is given in Table I.

Deprotonation and Dehydrogenation of I: Preparation of $[(\mu\text{-H})Fe_3(CO)_9(CCH_2)]^-$ (III). Although a number of bases were tried, two proved to be convenient for preparing this anion from I. The potassium salt of III was obtained by deprotonation with potassium acetate by the following procedure. In a typical reaction, 0.035 g (0.08 mmol) of I was dissolved in 20 mL of acetone. This yellow solution was transferred to another flask containing a suspension of $K[CH_3COO]$ (0.10 g, 0.104 mmol) in 3 mL of acetone. Stirring for 20 min at 25 °C resulted in a dark red solution and the evolution of 2.1 mL (0.082 mmol, 25 °C, 1 atm) of gas. An average of three runs gave 1.2 mmol of H_2 produced/mmol of I. GC analysis of the gas produced showed only the presence of H_2 although small amounts of CO cannot be excluded. Filtration was followed by removal of volatiles, including acetic acid, on a vacuum line. The yield of III was 0.33 g (0.07 mmol). The spectroscopic properties were the same as those reported by Mathieu et al.;[10] however, the ^1H NMR data for three derivatives are given in Table IX.

The second method employed $N(C_2H_5)_3$ as deprotonating agent. In a typical reaction, 0.33 g (0.07 mmol) was dissolved in 3.0 mL of hexane and 0.031 mL (0.22 mmol) of $N(C_2H_5)_3$ added at 25 °C. A reddish brown precipitate appeared within the first 5 min, and after 1 h the hexane was colorless. Removal of the supernatant hexane followed by drying under vacuum yielded 0.037 g (0.07 mmol) of the $[HN(C_2H_5)_3]^+$ salt of III.

Protonation and Hydrogenation of III. Although some I is produced with sequential protonation and hydrogenation of III, highest yields were obtained for simultaneous protonation and hydrogenation under a continuous purge of H_2 (see discussion above). In a typical reaction, 0.15 g (0.32 mmol) of III was suspended in 15 mL of hexane. H_2 gas was admitted to the solvent via a gas dispersion frit establishing a slow purge. The mixture was sonicated briefly to further disperse the solid, and 10 mL of H_3PO_4 (85% in H_2O) was added. In about 20 min the acid layer was colorless and the hexane layer turned a deep orange yellow. ^1H NMR of the material in the hexane solution showed a mixture of I and II. Centrifugal chromatography with hexane yielded 0.10 g (0.22 mmol) of I (72%).

Protonation of III at 25 °C yielded II and another compound in a ratio of about 3:1. The ^1H NMR of this species ($(C_6D_6$, 20 °C) δ 4.46 (2 H), −19.4 (1 H), −26.4 (1 H)) when compared to that of $H_2Os_3(CO)_9CCH_2$[35] suggests the formation of $H_2Fe_3(CO)_9CCH_2$ (IV). Protonation with CF_3COOH at −60 °C yields IV in above 90% yield (by ^1H NMR). Reaction of a sample of IV with CO (10 min, 25 °C, 1 atm) yielded II. Reaction of IV with H_2 (10 min, 25 °C, 1 atm) resulted in the formation of I.

Labeling Studies. The ^{13}C-enriched compounds were prepared from enriched $Fe(CO)_5$ (25–30% by IR) in turn prepared by published methods.[50] In this case the formyl complex, $[(CO)_4FeC(O)H]Na$[51] was reduced with BH_3·THF. The yields of I were lower than indicated above but sufficient. The reaction of I with ^{13}CO was carried out under the same conditions as described for the equilibrium measurements except that the pressure used was 1 atm.

For the protonation/hydrogenation reactions, the procedures used were the same as described above except that D_3PO_4 (85% in D_2O) and D_2 were used. Those runs in which a "delay" time was introduced involved complete protonation in the absence of hydrogen followed by removal of the hexane layer to a separate vessel. After a specified period of time, hydrogen was bubbled through the solution and the products were analyzed.

In the case of the mass spectrometric analysis of the gases evolved in the deprotonation of $I(D_2)$, the following modifications in procedures were employed. Acetone (5 mL) was frozen on a sample of 0.15 mmol of $I(D_2)$ in a 25-mL flask at −196 °C on a vacuum line. This was followed with 0.44 mmol of $N(C_2H_5)_3$ after which the flask with contents still frozen was attached to the gas inlet of the mass spectrometer. The flask was warmed, and reaction was allowed to take place at 23 °C for 20 min after which period the contents were again frozen at −196 °C. The noncondensable gases were then directly sampled into the mass spectrometer. The spectrometer was calibrated with a known mixture of D_2/H_2 as well as H_2.

Kinetics of the Deprotonation of I. The dependence of the rate of the deprotonation of I on concentration of $N(C_2H_5)_3$ and I was examined by observing the time dependence of the concentration of I under pseudo-first-order conditions at 25 °C. Reactions were carried out in a conventional Schlenk flask immersed in a water bath. Concentrations of I were measured by using quantitative infrared spectroscopy (2062 cm^{-1}) and were in the range 0.1–0.6 mM. Concentrations of $N(C_2H_5)_3$ were 10–25 times larger. Under these conditions reaction half-lives were ca. 10 min. Samples were withdrawn with a syringe through the side arm of the flask during the course of the reaction and were immediately analyzed. A single run of $(\mu\text{-H})_3Fe_3(CO)_9(\mu_3\text{-}CCH_2C_6H_5)$ with a 33-fold excess of $N(C_2H_5)_3$ was used to obtain the relative rate constant for the benzyl derivative. Rate constants were calculated with least-squares procedures.

The rate of H_2 gas evolution on the deprotonation of I with $N(C_2H_5)_3$ was measured by using a microvolumeter[52] directly attached to a 50-mL modified, spherical Schlenk vessel immersed in a water bath. Concentrations of I were about 5 mM and those of $N(C_2H_5)_3$ ranged from 1 to 5 times larger.

Reaction of III with Phosphine under Acid Conditions. In a typical reaction, 22.2 μL (0.22 mmol) of $Ph(CH_3)_2P$ was added to 0.04 g (0.07 mmol) of the $[HN(C_2H_5)_3]^+$ salt of III in benzene. After 20 min this was followed with 5 mL of H_3PO_4, and the reaction was stirred for 30 min at 25 °C during which period the benzene layer turned dark brownish red. At this point the ^1H NMR showed the presence of II and a second product. After solvent was removed, the product mixture was sublimed at 25 °C under high vacuum. Compound II sublimed away leaving the other product in the residue. The latter was dissolved in a minimum of toluene, and a compound identified as $(\mu\text{-H})Fe_3(CO)_9(\mu\text{-CO})[Ph(CH_3)_2P](CCH_3)$ was obtained as red-brown crystals after cooling: MS, p^+ 585.850 measd, 585.852 calcd, loss of nine CO's observed; IR (hexane, cm^{-1}) 2090 (w), 2055 (m), 2040 (m), 2005 (s), 1940 (w), 1860 (br, w); ^1H NMR (C_6D_6, 20 °C) δ 6.98–7.32 (m, 5 H, Ph), 4.20 (s, 3 H, CCH_3), 1.20 (m, 6 H, $Ph(CH_3)_2P$), −18.99 (s, 1 H, FeHFe); $^{31}P\{^1H\}$ NMR δ 27.22 (s).

Acknowledgment. The support of the National Science Foundation under Grant CHE 8408251 is gratefully acknowledged. We thank Dr. C. E. Housecroft for aid with the NMR studies and Dr. G. B. Jacobsen for the preliminary work on the vinylidene cluster. We thank Dr. J. B. Keister for several preprints and helpful comments.

Registry No. I, 69440-00-2; I (^{13}CO), 109787-08-8; I (D_2), 109787-09-9; I (R = CH_3), 69440-01-3; I (R = C_2H_5), 69440-02-4; I (R = C_3H_7), 109787-03-3; I′, 102774-25-4; II, 88610-52-0; II (^{13}CO), 109800-95-5; II (D), 109787-00-0; II (R = CH_3), 109787-04-4; II (R = C_2H_5), 109787-05-5; II′, 109838-63-3; III $[HN(C_2H_5)_3]$, 109787-02-2; III (K), 99725-90-3; III$^-$ (R = CH_3), 109787-06-6; III$^-$ (R = C_6H_5), 102774-26-5; IV, 109787-07-7; $[(CO)_4FeC(O)CH_3]Na$, 64867-63-6; $Fe(CO)_5$, 13463-40-6; $Na[Fe(CO)_4C(O)C_6H_5]$, 71357-09-0.

(50) Noack, K.; Ruch, M. *J. Organomet. Chem.* **1969**, *17*, 309.
(51) Winter, S. R.; Cornett, G. W.; Thompson, E. A. *J. Organomet. Chem.* **1977**, *133*, 339.
(52) Davis, D. D.; Stevenson, K. L. *J. Chem. Educ.* **1977**, *54*, 394.